Autoencoder-based Pilot Pattern Design for CDL Channels

Yuta Yamada
Graduate School of Science and Technology
Keio University
Yokohama, Japan
y.yamada@ohtsuki.ics.keio.ac.jp

Tomoaki Ohtsuki
Department of Computer and Information Science
Keio University
Yokohama, Japan
ohtsuki@ics.keio.ac.jp

***Abstract*—In the pilot-based channel estimations, a large number of pilot signals enable an improvement in the channel estimation accuracy but force a decrease in the data transmission efficiency. Therefore, the pilot pattern design schemes on the resource grid have been researched to achieve high channel estimation accuracy with a small number of pilot signals. In the conventional scheme for pilot pattern design, the autoencoder which enables discrete feature selection is utilized to design pilot patterns for Vehicular-A channels. However, the pilot pattern for other channels is not reported, and it is not clear whether this scheme has good performance compared to uniform pilot patterns. In this paper, we derive the pilot patterns for Clustered Delay Line (CDL) channels specified in the 5th Generation Mobile Communication System (5G) standard using the autoencoder-based pilot pattern design scheme. We also derive the pilot patterns for CDL-A and CDL-D, which model respectively NLOS (Non-Line-of-Sight) and LOS (Line-of-Sight) environments, with different three speeds of User Equipment (UE). Through computer simulation, we show that the autoencoder-based pilot patterns improve the channel estimation accuracy compared to the uniform pilot pattern.**

***Index Terms*—Channel Estimation, Deep Learning, Feature Selection**

I. Introduction

In wireless communications, accurate downlink channel state information (CSI) is needed to improve the quality of communications for users and estimate the transmitted symbols from the received symbols. In frequency division duplex (FDD) systems, which enable to improve the coverage and reduce the interference, the reciprocity of the uplink and downlink channels does not exist. Therefore, the downlink channel estimation at the user equipment (UE) is regarded as one of the essential components for FDD systems [1]. In general channel estimation methods, the pilot signals which are known between the transmitter and the receiver are used. A large number of pilot signals improve the accuracy of channel estimation but degrades the data transmission efficiency because the pilot signals consume wireless resources without useful information transmission [2], [3]. Therefore, not only accurate channel estimation but also the informative pilot design is important to reduce the pilot's overhead while keeping the channel estimation accuracy [4], [5].

Regarding pilot pattern design, in [6], the pilot pattern design scheme using the concrete autoencoder (CAE) [7], that enables discrete feature selection, was proposed, and pilot patterns that improve the channel estimation accuracy was derived for Vehcular-A channels. However, the pilot pattern for other channels is not reported, and it is not clear whether this scheme has good performance compared to uniform pilot patterns.

In this paper, we derive the CAE-based pilot pattern for a cluster delay line (CDL) channel specified in the 5th Generation Mobile Communication System (5G) standard [8]. We also derive the pilot patterns for CDL-A and CDL-D, which model respectively Non-Line-of-Sight (NLOS) and Line-of-Sight (LOS) environments, with different three speeds of UE (User Equipment). Through computer simulation, we show that the CAE-based pilot patterns improve the channel estimation accuracy compared to the uniform pilot pattern. We also evaluate the pilot pattern and channel estimation accuracy based on the existence of LOS paths and the speed of UE. As a result, we also show the CAE-based pilot patterns improve the channel estimation accuracy compared to the uniform pilot pattern in both NLOS and LOS environments with three UE's speeds.

The rest of this paper is organized as follows. In Section II, we present the system model and the traditional channel estimation schemes. In Section III, we introduce the CAE-based pilot pattern design scheme used by this research. Section IV provides the simulation results, and Section V concludes this paper.

II. System Model

Fig. 1 shows the system model. We consider that BS and UE are equipped with a uniform rectangular array (URA) with N_t antenna elements and N_r antenna elements, respectively. The transmitter and the receiver utilize OFDM over M subcarriers. The pilot domain length along the time grid is K time slots. The observed signal of the receiver side at the m th subcarrier and the k th time slot $\mathbf{y}[m,k] \in \mathbb{C}^{N_r \times 1}$ can be modeled as,

$$\mathbf{y}[m,k] = \mathbf{H}[m,k] \cdot \mathbf{x}[m,k] + \mathbf{n}[m,k] \ (m \in [1,\ M], k \in [1,\ K]) \tag{1}$$

where $\mathbf{H}[m,k] \in \mathbb{C}^{N_r \times N_t}$ and $\mathbf{x}[m,k] \in \mathbb{C}^{N_t \times 1}$ denote the MIMO downlink fading channel at the m th subcarrier and the k th time slot and the transmitted OFDM symbol. $\mathbf{n}[m,k] \in \mathbb{C}^{N_r \times 1}$ is the complex additive white Gaussian noise (AWGN) at the m th subcarrier and the k th time slot, and

$\mathbf{n}[m,k] \sim \mathcal{CN}(0,\sigma_n^2)$ with variance σ_n^2, which is independent across subcarriers and time slots.

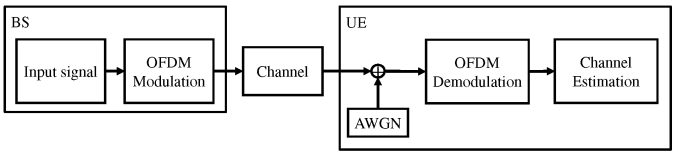

Fig. 1. The system model.

In the pilot-based channel estimation, the received signal at the pilot location (m_p, k_p) can be re-modeled as,

$$\mathbf{y}[m_p,k_p] = \mathbf{H}[m_p,k_p]\cdot\mathbf{x}[m_p,k_p] + \mathbf{n}[m_p,k_p],\ (m_p,k_p)\in\Omega_p \tag{2}$$

where $\mathbf{x}[m_p,k_p]$ is the pilot signal at the pilot location (m_p,k_p). Ω_p is the collection of all the pilot locations, and $N_p = |\Omega_p|$ is the number of pilot locations. In least square (LS) and minimum mean squared error (MMSE) estimation with eq. (2), the estimated channel at the pilot locations can be given respectively as [11],

$$\mathbf{h}^{LS}[m_p,k_p] = \mathbf{y}[m_p,k_p]\cdot\mathbf{x}^{+}[m_p,k_p] \tag{3}$$

$$\mathbf{H}^{MMSE}[m_p,k_p] = \mathcal{R}_{\mathbf{H}\mathbf{H}^{LS}}\cdot\mathcal{R}^{-1}_{\mathbf{H}^{LS}}\cdot\mathbf{H}^{LS}[m_p,k_p] \tag{4}$$

where $\mathcal{R}_{\mathbf{H}^{LS}}$ and $\mathcal{R}_{\mathbf{H}\mathbf{H}^{LS}}$ denote the autocorrelation matrix of $\mathbf{H}^{LS}[m_p,k_p]$ and the cross-correlation matrix between the true channel matrix and the temporary channel matrix achieved by the LS estimation.

III. Pilot Design Scheme using Concrete Autoencoder

Fig. 2 shows the CAE architecture, which consists of a concrete selector layer as the feature selection layer and a decoder neural network (NN) as the reconstruction function. CAE is an autoencoder whose latent variables $\boldsymbol{u}$ selected by a concrete selector layer follow a categorical distribution. A concrete selector layer has k neurons, and the number of nodes k, which also represents the number of latent features, is user-specified. The details of training the CAE is shown in Algolithm 1. The weight vector $\boldsymbol{m}^{(i)} \in \mathbb{R}^{d\times 1}$ for the neuron i of the concrete selector layer follow the Concrete distribution, which is defined by the random variables of the categorical distribution $\boldsymbol{\alpha}^{(i)}$ and the temperature parameter T [9]. In training, the random variables of the categorical distribution $\boldsymbol{\alpha}^{(i)}$ and the weight of the decoder θ. Finally, the temperature parameter T becomes 0, and the weight vector $\boldsymbol{m}^{(i)}$ also becomes one-hot vector. This CAE training algorithm enables the discrete feature selection

Fig. 3 shows the CAE-based pilot pattern design network [6]. The pilot pattern design network learns the pilot locations and the interpolation network to estimate the channel response in all of the resource grids from the LS channel estimates with high accuracy In detail, the selector layer which enables

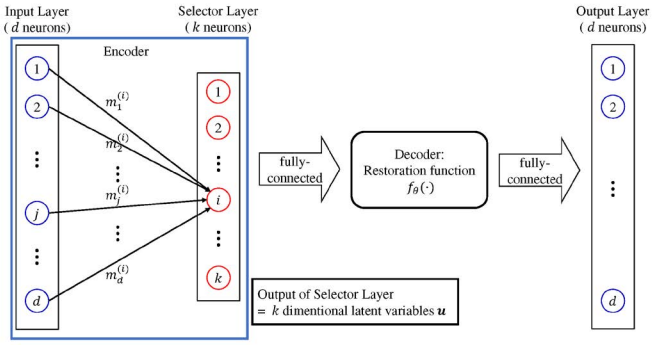

Fig. 2. The concrete autoencoder (CAE) architecture.

Algorithm 1 : The pseudocode training the concrete autoencoder.

Input:
$\boldsymbol{X}\in\mathbb{R}^{n\times d}$: training dataset, k: the number of selected features,
$f_\theta(\cdot);\theta$: decoder network,
λ: learning rate, B: the number of epochs, T_0: initial temprature, T_B: final temprature

Initialize:
$\alpha^{(i)}$: small positive values for $1\le i\le k$
θ: a standard initialization for the decoder network
for $b\in[1,B]$ **do**
Let $T = T(b) = T_0(T_B/T_0)^{b/B}$
for $i\in[1,k]$ **do**
Sample the weights of selector layer $\boldsymbol{m}^{(i)}$
Let the latent variable $\boldsymbol{U}^{(i)} = \boldsymbol{X}\cdot\boldsymbol{m}^{(i)}$
end for
Define the latent variable matrix $\mathbf{U}\in\mathbb{R}^{n\times k}$ by concatenating $\mathbf{U}^{(1)},\cdots,\boldsymbol{U}^{(i)}\cdots\boldsymbol{U}^{(k)}$
Compute the loss $L = ||f_\theta(\boldsymbol{U};\theta)-\boldsymbol{X}||_2$
Compute the gradient of the loss with regard to θ using back propagation
Compute the gradient of the loss with regard to $\boldsymbol{\alpha}^{(i)}$ using the reparameterization trick
Update the parameters $\theta\leftarrow\theta-\lambda\nabla_\theta L$ and $\alpha^{(i)}\leftarrow\boldsymbol{\alpha}^{(i)}-\lambda\nabla_{\boldsymbol{\alpha}^{(i)}}L$ for $1\le i\le k$
end for

Output:
f_{θ^*}: trained reconstruction network, $\boldsymbol{\alpha}^{(i)}$: trained concrete parameter
$\boldsymbol{M}^* = [\boldsymbol{m}^{(1)},\cdots,\mathbf{m}^{(i)},\cdots,\boldsymbol{m}^{(k)}]\in\mathbb{R}^{d\times k}$: weight of trained reduction network

the discrete feature selection learns the pilot locations which contribute to the channel estimation accuracy as features. That is to say, the number of the concrete selector layer's neurons k, which represents the number of dimensions of the latent space, equals the number of pilot signals N_p. The decoder which is the reconstruction function learns the relation between the LS channel estimates and the perfect channel response in all of the resource grids.

IV. Simulation Results

A. Simulation Specifications

In this section, we show the proposed pilot patterns for CDL channels derived by CAE and evaluate the channel estimation accuracy of the CAE-based pilot patterns and the uniform patterns. The parameters of the wireless environment are listed

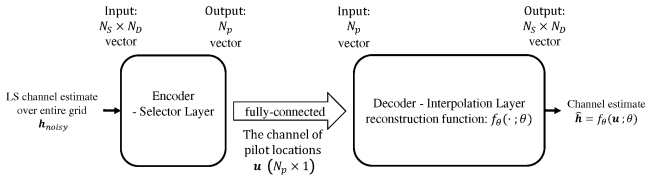

Fig. 3. The CAE-based pilot pattern design network.

in Table I. To evaluate the performance of the CAE-based pilot pattern design scheme for the CDL channel, we consider a single-input single-output (SISO) system, in which both a BS and a UE have a single isotropic antenna. The CDL-A and CDL-D channels are modeled as NLOS environments and LOS environments, respectively. The uplink and downlink carrier frequencies are 2.0 GHz and 2.1 GHz, respectively. The number of subcarriers M equals 72, and the subcarrier spacing (SCS) is set as 15 kHz. The number of pilot domain's time slots K equals 14, so the size of the time-frequency resource grid is set as 72×14.

The parameters of training NN are listed in Table II, and Fig. 4 shows the structure of the CAE's decoder. To train the network, we generated the 180,000 noisy channel samples for training, which covers the SNR of -3 to 30 dB with 3 dB step size to get enough performance with a single network for a wide range of SNR. In other words, the training dataset contains 15,000 noisy channel samples at 12 different SNRs. The validation dataset consists of about 4,000 noisy channel samples selected randomly from a dataset containing 40,000 noisy channel samples. The SNR of the validation noisy samples is set to 30 dB as the target SNR. The testing dataset contains 100,000 samples at the SNR of -5 to 30 dB with 5 dB step size. In the test, the testing dataset is divided into ten parts randomly, and the average of mean squared error (MSE) for each part is used as a result. For the decoder of the CAE, we have used three dense layers with LeakyReLU(0.2) activation and Dropout(0.1).

We use the MSE as the channel estimation accuracy, defined by

$$MSE = \frac{1}{MKN_D} \sum_{d=1}^{N_D} ||\mathbf{H}_{ideal}^{(d)} - \hat{\mathbf{H}}^{(d)}||_2^2 \ , \qquad (5)$$

where N_D denotes the size of the test dataset. Moreover, to investigate the bias of the allocated pilots on the resource grid, we use the mean and standard deviation of the distance between pilots along the frequency (subcarriers) axis and the time (time slots) axis, respectively.

B. Evaluation

Fig. 5 shows the pilot patterns for CDL-A and CDL-D channels with $v = 50$ km/h. Table III provides the mean and standard deviation of the distance between pilots for the CDL-A and the CDL-D channels with $v = 50$ km/h. In Table III, the elements represent (mean distance, standard deviation of the distance). The pilot signals for CDL-D are allocated more equally on the resource grid than for CDL-A. According to Table III, the mean pilot distance and the standard derivation of the distance along the subcarrier axis for CDL-A is larger than those for CDL-D, respectively. It is thought that this is because the frequency response of the CDL-A channels varies more than that of the CDL-D channels.

Figs. 6 and 7 show the MSE for CDL-A and CDL-D channels with the speed of UE $v = 50$ km/h, respectively. In both CDL-A and CDL-D channels where the SNR was higher than 5 dB, the CAE-based pilot pattern improves the MSE compared to the

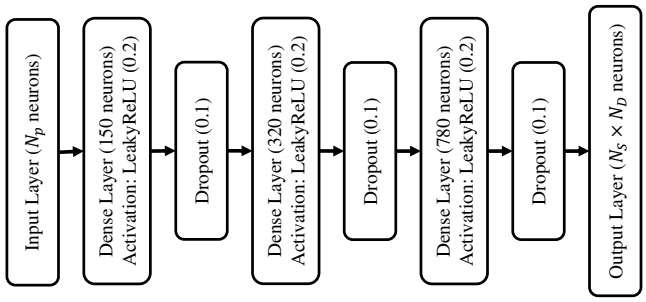

Fig. 4. The decoder network of CAE.

TABLE I
THE PARAMETERS OF CHANNELS.

Parameter	Value
Channel model	CDL-A / CDL-D
Carrier Frequency (uplink)	2.0 GHz
Carrier Frequency (downlink)	2.1 GHz
The number of subcarriers M	72
Subcarrier spacing	15 kHz
The number of pilot domain's time slots K	14
Antenna elements	isotropic
The number of transmit antennas N_t	1
The number of receive antennas N_r	1
The number of pilots N_p	8, 16, 48
Speed of UE v	4, 50, 80 km/h

TABLE II
THE PARAMETERS FOR TRAINING THE NEURAL NETWORK.

Parameter	Value
Size of training dataset	180,000
Size of validation dataset	about 4,000
Size of testing dataset M	100,000
Learning rate	0.001
The number of epochs	100
Batch size	128
Loss function	mean squared error
Optimizer	Adam

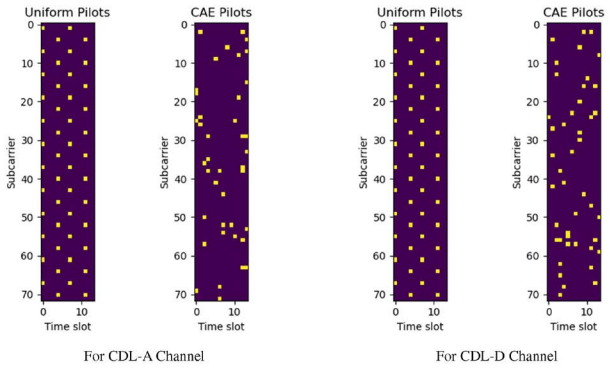

Fig. 5. The pilot patterns for CDL-A and CDL-D channels with $v = 50$ km/h ($N_p = 48$).

TABLE III
THE MEAN AND STANDARD DEVIATION OF THE DISTANCE BETWEEN ALLOCATED PILOTS FOR CDL-A AND CDL-D ($N_p = 48$). THE ELEMENTS REPRESENT (MEAN DISTANCE, STANDARD DEVIATION OF THE DISTANCE).

	along subcarrier axis	along time-slot axis
CDL-A	$(16.75, 15.91)$	$(4.140, 3.044)$
CDL-D	$(13.79, 11.25)$	$(4.909, 3.528)$

uniform pilot pattern for any number of pilots. In addition, the improvement in MSE due to the increase in the number of pilots is greater for the CDL-A channel than for CDL-D channel.

Figs. 8 and 9 show the derived pilot pattern for CDL-A and CDL-D channels respectively with the speed of UE $v = 4,\ 50,\ 80$ km/h. Figs. 10 and 11 show the MSE of CAE-based and uniform pilot patterns for the CDL-A and CDL-D channels respectively with the speed of UE v at SNR $= 30$ dB. Tables IV and V list the mean and standard deviation of the distance between pilots for CDL-A and CDL-D channels respectively with $v = 4,\ 50,\ 80$ km/h. In Tables IV and V, the elements represent (mean distance, standard deviation of the distance). According to Tables IV and V, compared with the uniform pilot pattern, in the derived pilot patterns for CDL-A channels, the mean distance between pilots along the subcarrier axis is large, and the mean distance between pilots along the time-slot axis is small. According to Fig. 10 and 11, the CAE-based pilot pattern improves the MSE of channel reconstruction even in environments with any speed of UE.

Considering the results of the MSE and the pilot pattern analysis, the pilot patterns that improve the MSE for both the CDL-A and the CDL-D channels are the patterns where the pilot distance along the subcarrier axis is large, and the pilot distance along the time-slot axis is small. In the case of the CDL-A channels, as the speed of UEs increases, the mean pilot distance along the subcarrier axis is small, and that along the time-slot axis is large. Therefore, more dense pilot

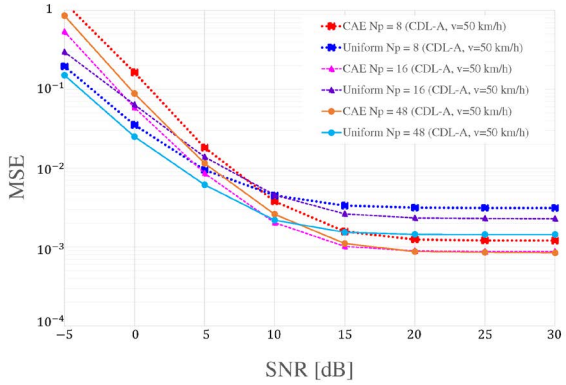

Fig. 6. MSE vs. SNR of CDL-A channel with $v = 50$ km/h.

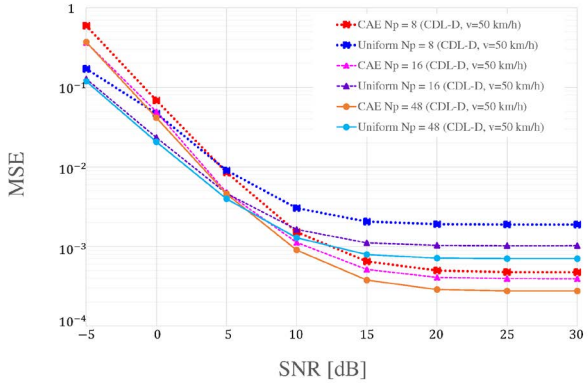

Fig. 7. MSE vs. SNR of CDL-D channel with $v = 50$ km/h.

TABLE IV
THE MEAN AND STANDARD DEVIATION OF THE DISTANCE BETWEEN ALLOCATED PILOTS FOR THE CDL-A CHANNELS WITH $v = 4,\ 50,\ 80$ km/h ($N_p = 48$). THE ELEMENTS REPRESENT (MEAN DISTANCE, STANDARD DEVIATION OF THE DISTANCE).

	along subcarrier axis	along time-slot axis
$v = 4$ km/h	$(18.70,\ 15.49)$	$(2.700,\ 1.735)$
$v = 50$ km/h	$(16.75,\ 15.91)$	$(4.140,\ 3.044)$
$v = 80$ km/h	$(15.60,\ 14.21)$	$(5.667,\ 3.197)$
Uniform	$(6.000,\ 0.000)$	$(7.000,\ 0.000)$

patterns along the subcarrier axis are derived as the UEs' speed increases. On the other hand, in the case of the CDL-D channels, comparing small UE's speed ($v = 4$ km/h)) and large UE's speed ($v = 50,\ 80$ km/h)), the mean pilot distance along the subcarrier axis and the time-slot axis is large in large UE's speed situation.

V. CONCLUSION

In this paper, we have derived the pilot patterns for the CDL channels using the autoencoder-based pilot pattern design scheme. In this scheme, the autoencoder called CAE, which

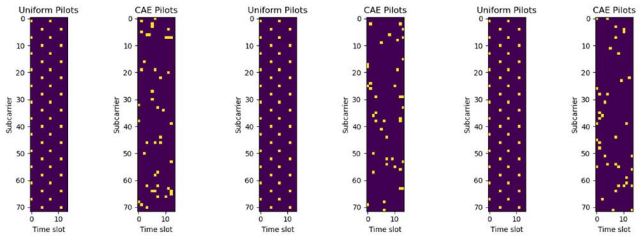

Fig. 8. The pilot patterns for the CDL-A channels with $v = 4,\ 50,\ 80$ km/h ($N_p = 48$)

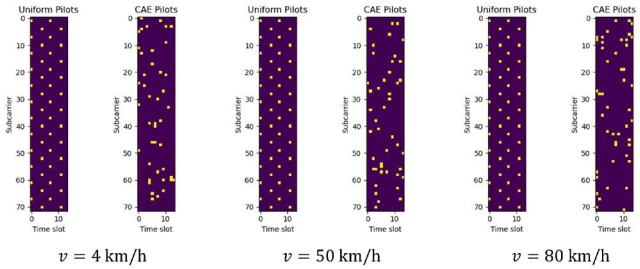

Fig. 9. The pilot patterns of the CDL-D channels with $v = 4,\ 50,\ 80$ km/h ($N_p = 48$).

TABLE V
THE MEAN AND STANDARD DEVIATION OF THE DISTANCE BETWEEN ALLOCATED PILOTS FOR THE CDL-D CHANNELS WITH $v = 4,\ 50,\ 80$ km/h ($N_p = 48$). THE ELEMENTS REPRESENT (MEAN DISTANCE, STANDARD DEVIATION OF THE DISTANCE).

	along subcarrier axis	along time-slot axis
$v = 4$ km/h	(12.03, 11.55)	(3.625, 2.546)
$v = 50$ km/h	(13.79, 11.25)	(4.909, 3.528)
$v = 80$ km/h	(13.26, 11.62)	(4.636, 3.227)
Uniform	(6.000, 0.000)	(7.000, 0.000)

enables the discrete feature selection, is utilized for the pilot pattern design. In the training phase, we set the target SNR for the validation data and define the validation loss for the data of the target SNR to exploit the pilot pattern adapted to various noisy environments. Simulation results show that the CAE-based pilot pattern improves channel estimation accuracy compared to the uniform pilot pattern. We also derive and evaluate the pilot patterns and their channel estimation accuracy based on the existence of LOS paths (CDL-A or CDL-D) and the speed of UE ($v = 4,\ 50,\ 80$ km/h). As a result, for the speed of UE $v = 4,\ 50,\ 80$ km/h in both the CDL-A channel and the CDL-D channel, we also show that the CAE-based pilot pattern improved the channel estimation accuracy compared to the uniform pilot pattern.

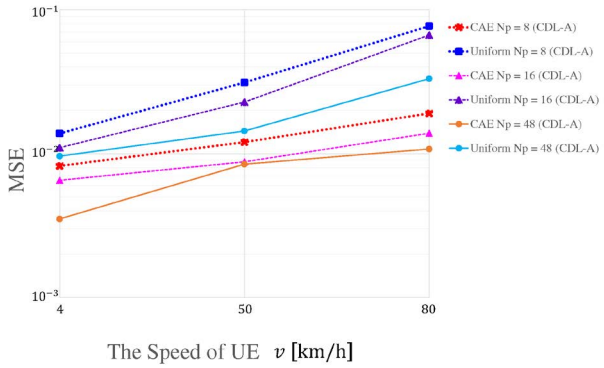

Fig. 10. MSE vs UE's speed of the CDL-A channels (SNR = 30 dB).

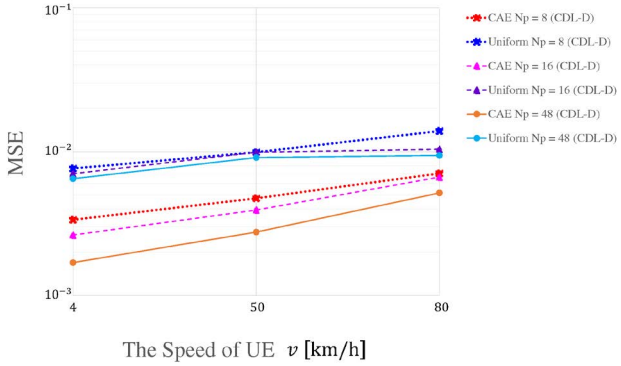

Fig. 11. MSE vs UE's speed of the CDL-D channels (SNR = 30 dB).

REFERENCES

[1] E. Bjornson, E. G. Larsson, and T. L. Marzetta, "Massive MIMO: ten myths and one critical question," *IEEE Commun. Mag.*, vol. 54, no. 2, pp. 114-123, Feb 2016.

[2] H. Bergaoui, Y. Mlayeh and F. Tlili, "Adaptive Pilot Pattern for Massive MIMO Systems," *IEEE Access*, vol. 9, pp. 81115-81124, 2021.

[3] R. M. Rao, V. Marojevic and J. H. Reed, "Adaptive Pilot Patterns for CA-OFDM Systems in Nonstationary Wireless Channels," *IEEE Trans. Veh. Technol.*, vol. 67, no. 2, pp. 1231-1244, Feb. 2018.

[4] M. B. Mashhadi and D. Gunduz, "Pruning the Pilots: Deep Learning-Based Pilot Design and Channel Estimation for MIMO-OFDM Systems," *IEEE Trans. Wirel. Commun.*, vol. 20, no. 10, pp. 6315-6328, Oct. 2021.

[5] X. Ma and Z. Gao, "Data-Driven Deep Learning to Design Pilot and Channel Estimator for Massive MIMO," *IEEE Trans. Veh. Technol.*, vol. 69, no. 5, pp. 5677-5682, May 2020.

[6] M. Soltani, V. Pourahmadi and H. Sheikhzadeh, "Pilot Pattern Design for Deep Learning-Based Channel Estimation in OFDM Systems," *IEEE Wireless Commun. Lett.*, vol. 9, no. 12, pp. 2173-2176, Dec. 2020.

[7] A. Abid, M. F. Balin, and J. Zou, "Concrete autoencoders for differentiable feature selection and reconstruction," arXiv Prepr. arXiv1901.09346, 2019.

[8] 3GPP TR 38.901. "Study on channel model for frequencies from 0.5 to 100 GHz, " 3rd Generation Partnership Project; Technical Specification Group Radio Access Network.

[9] C. J. Maddison, A. Mnih, and Y. W. Teh, "The Concrete Distribution: A Continuous Relaxation of Discrete Random Variables," arXiv Prepr. arXiv:1611.00712, 2016.

[10] Q. Shi, Y. Liu, S. Zhang, S. Xu, and V. K. N. Lau, "A Unified Channel Estimation Framework for Stationary and Non-Stationary Fading Environments," *IEEE Trans. Commun.*, vol. 69, no. 7, pp. 4937-4952, July 2021.

[11] Y. S. Cho, J. Kim, W. Y. Yang, and C. G. Kang, "Channel Estimation," *MIMO-OFDM Wireless Communications with MATLAB*, IEEE, pp.187-207, 2010.